Electronic Supplementary Information (ESI) for

Metal-organic framework derived trimetallic oxides with dual sensing functions for ethanol

Xin-Yu Huang,[a] Ya-Ru Kang,[b] Shu Yan,[a] Ahmed Elmarakbi,[c] Yong-Qing Fu*[c] and Wan-Feng Xie*[a, d]

[a] *College of Electronics and Information, University-Industry Joint Center for Ocean Observation and Broadband Communication, Qingdao University, Qingdao 266071, P. R. China.*

[b] *School of Integrated Circuits, University of Chinese Academy of Sciences, Beijing 100049, P. R. China.*

[c] *Faculty of Engineering and Environment, Northumbria University, Newcastle upon Tyne NE1 8ST, UK.*

[d] *Department of Physics, Dongguk University, Seoul 04620, South Korea.*

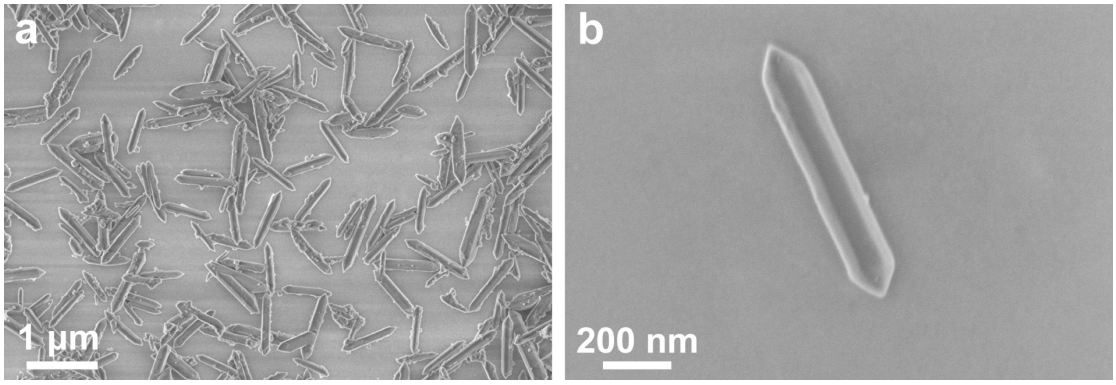

Fig. S1 FE-SEM images of the Fe-MIL-88B template with different resolutions.

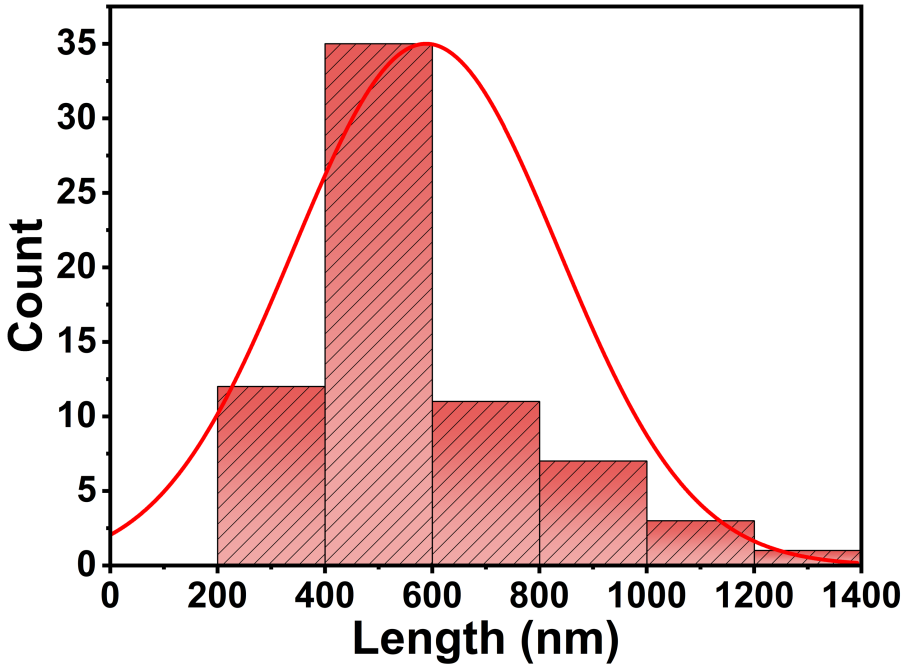

Fig. S2 Length distribution of elongated hexagonal rods of $Fe_7Co_{1.5}Ni_{1.5}$.

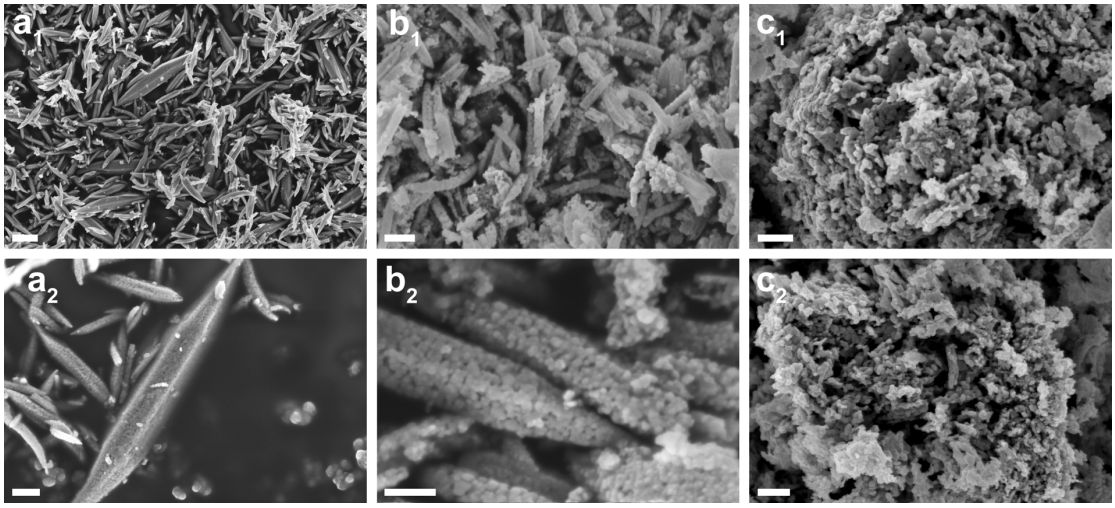

Fig. S3 SEM images of (a1, 2) $Fe_6Co_2Ni_2$, (b1, 2) $Fe_4Co_4Ni_2$, and (c1, 2) $Fe_2Co_6Ni_2$, respectively. Scale bar: 200 nm.

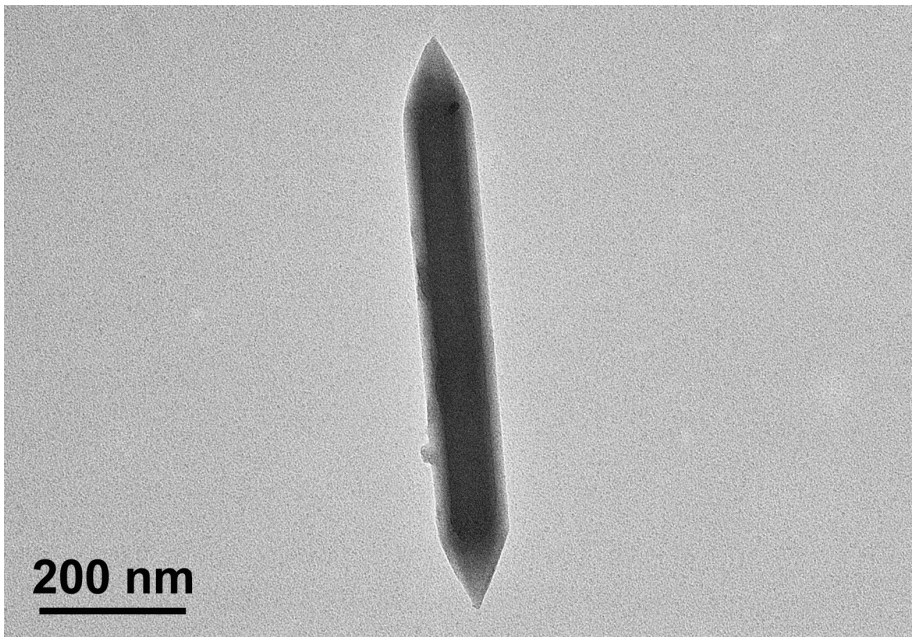

Fig. S4 TEM image of the Fe-MIL-88B template.

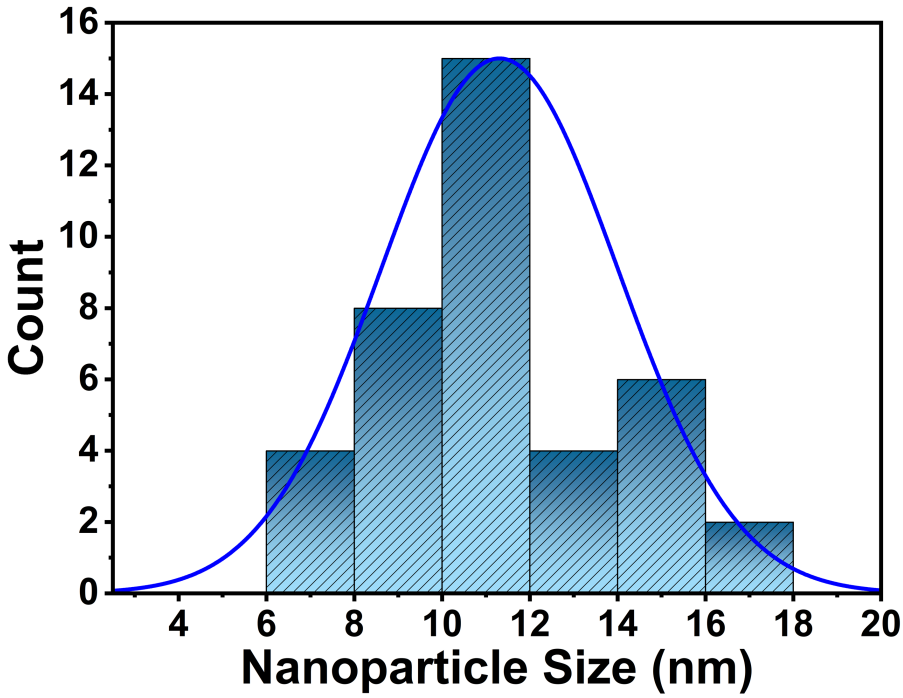

Fig. S5 Size distribution of nanoparticles of $Fe_7Co_{1.5}Ni_{1.5}$.

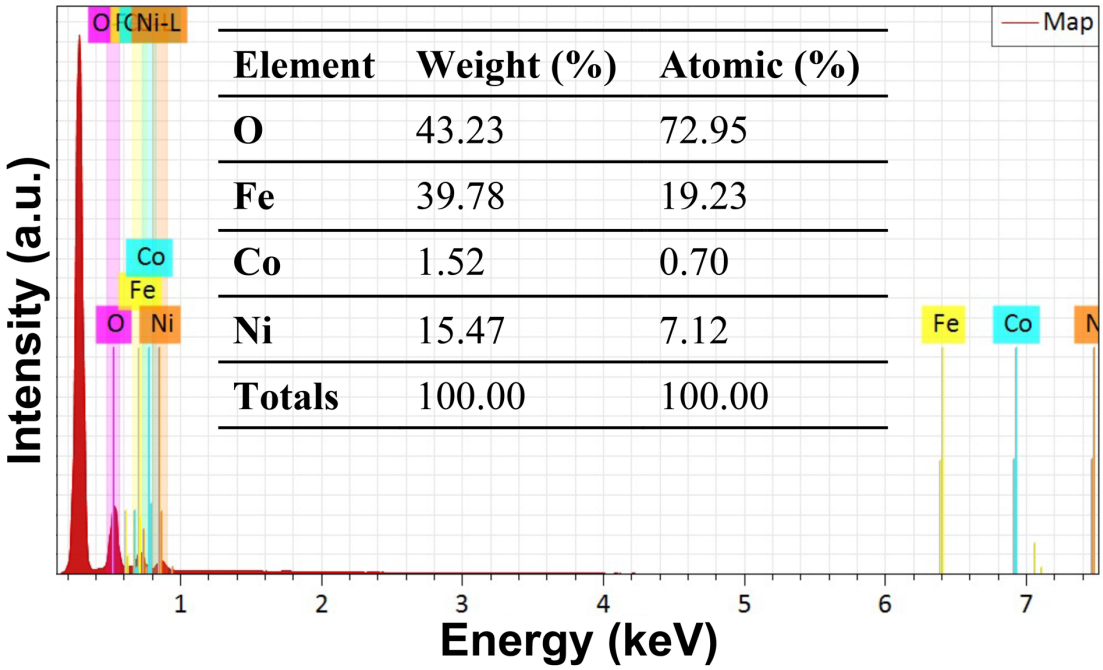

Element	Weight (%)	Atomic (%)
O	43.23	72.95
Fe	39.78	19.23
Co	1.52	0.70
Ni	15.47	7.12
Totals	100.00	100.00

Fig. S6 EDS spectrum and contents (inset) of $Fe_7Co_{1.5}Ni_{1.5}$.

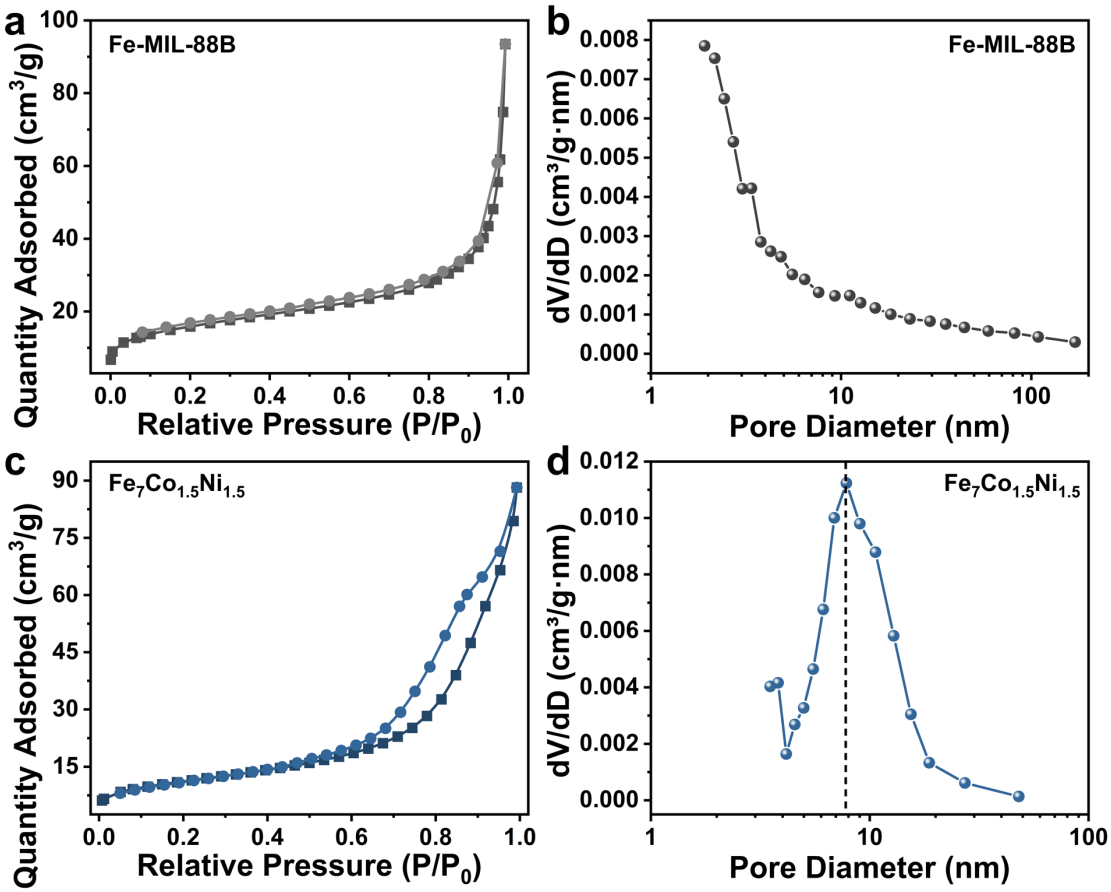

Fig. S7 N_2 adsorption-desorption isotherms of (a) Fe-MIL-88B and (c) $Fe_7Co_{1.5}Ni_{1.5}$, respectively. The corresponding pore diameter distribution of (b) Fe-MIL-88B (d) $Fe_7Co_{1.5}Ni_{1.5}$, respectively.

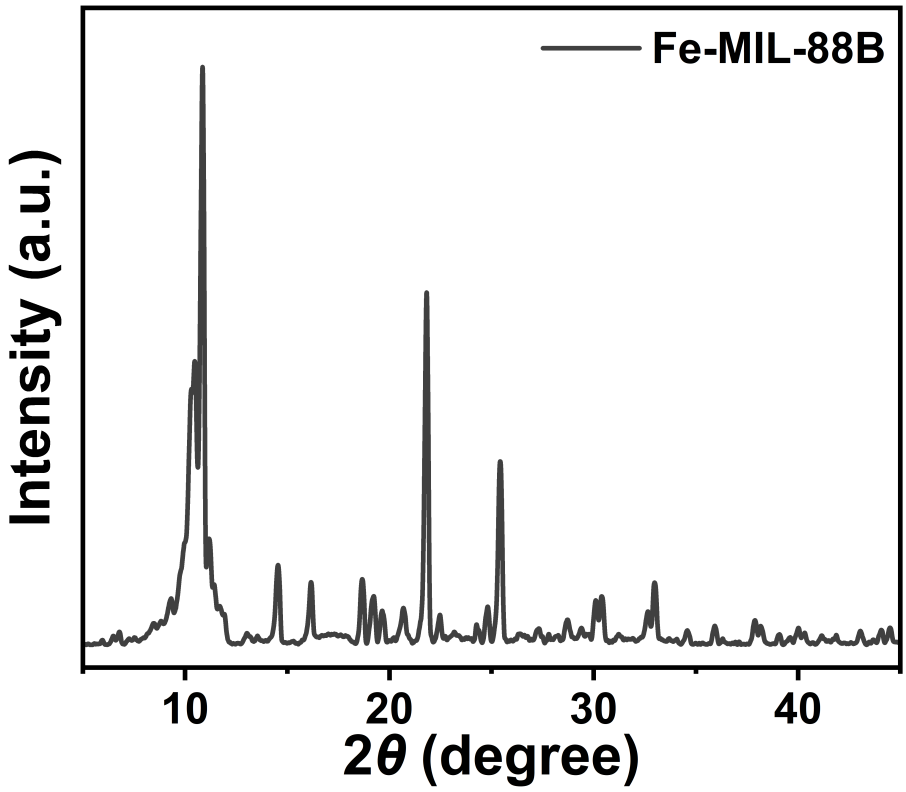

Fig. S8 XRD pattern of Fe-MIL-88B.

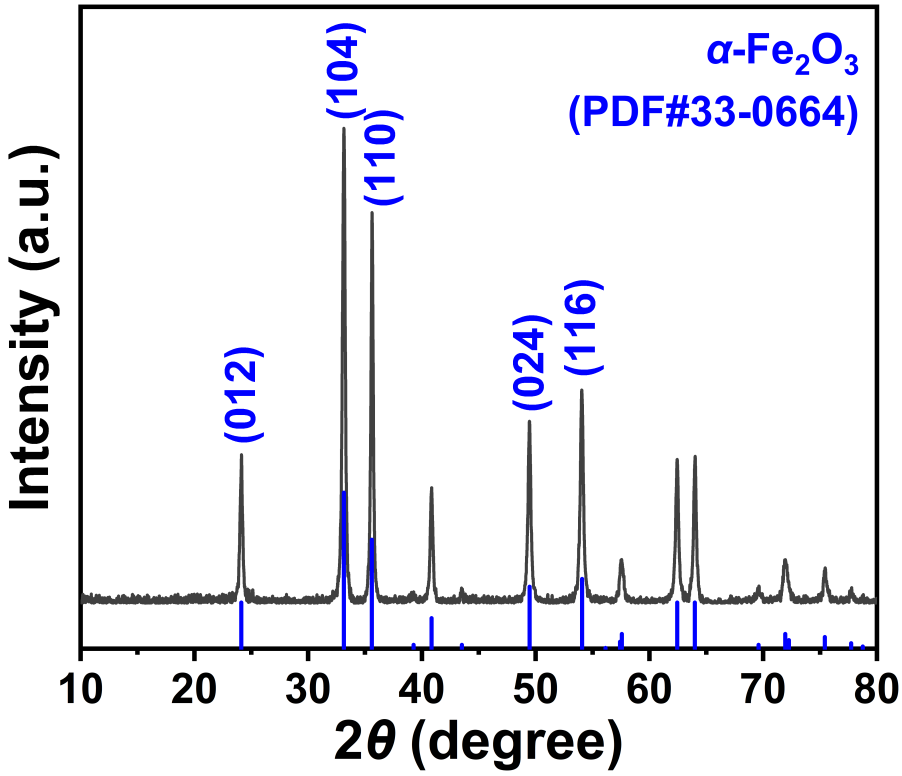

Fig. S9 XRD pattern of the pristine α-Fe_2O_3.

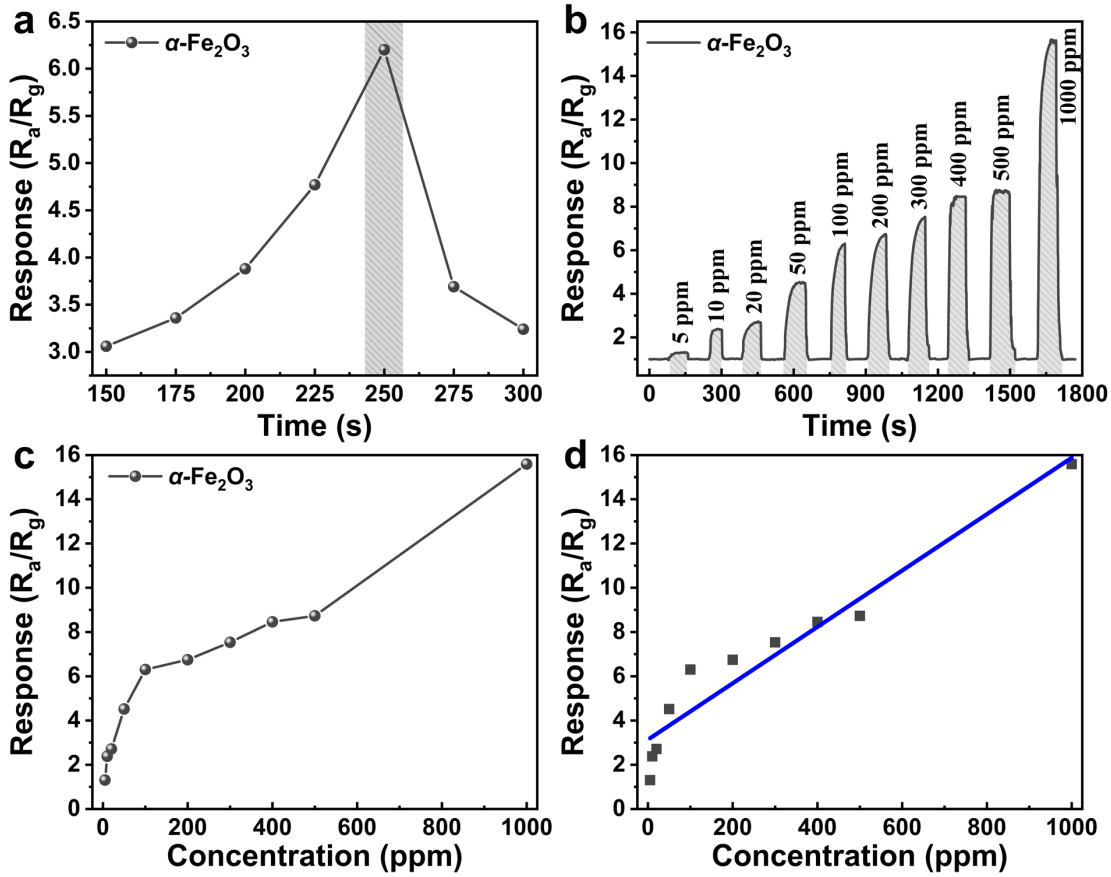

Fig. S10 (a) Responses of α-Fe_2O_3 towards 100 ppm ethanol at different operating temperatures. (b) The dynamic response curve of α-Fe_2O_3 towards different concentrations (from 5 to 1000 ppm) of ethanol at 250 °C. (c) The curve of responses *vs.* concentrations for α-Fe_2O_3. (d) The linear fitting of the response values as a function of ethanol concentrations.

Table S1 The crystal planes of α-Fe_2O_3, $CoFe_2O_4$, and $NiFe_2O_4$ correspond to the observed characteristic diffraction peaks.

Phase	2ϑ (degree)						
	24.14	33.10	35.66	40.86	49.46	54.12	57.42
α-Fe_2O_3 (PDF#33-0664)	(012)	(104)	(110)	(113)	(024)	(116)	(122)
Phase	2ϑ (degree)						
	18.24	30.06	35.45	43.47	53.89	57.39	62.73
$CoFe_2O_4$ (PDF#03-0864)	(111)	(220)	(311)	(400)	(422)	(511)	(440)
Phase	2ϑ (degree)						
	18.43	30.31	35.70	43.38	53.81	57.43	63.02
$NiFe_2O_4$ (PDF#54-0964)	(111)	(220)	(311)	(400)	(422)	(511)	(440)
Phase	2ϑ (degree)						
	18.84	31.00	36.52	38.20	44.30	58.72	66.48
$Co_{1.29}Ni_{1.71}O_4$ (PDF#40-1191)	(111)	(220)	(311)	(222)	(400)	(511)	(440)